

UCRL-JC-130155

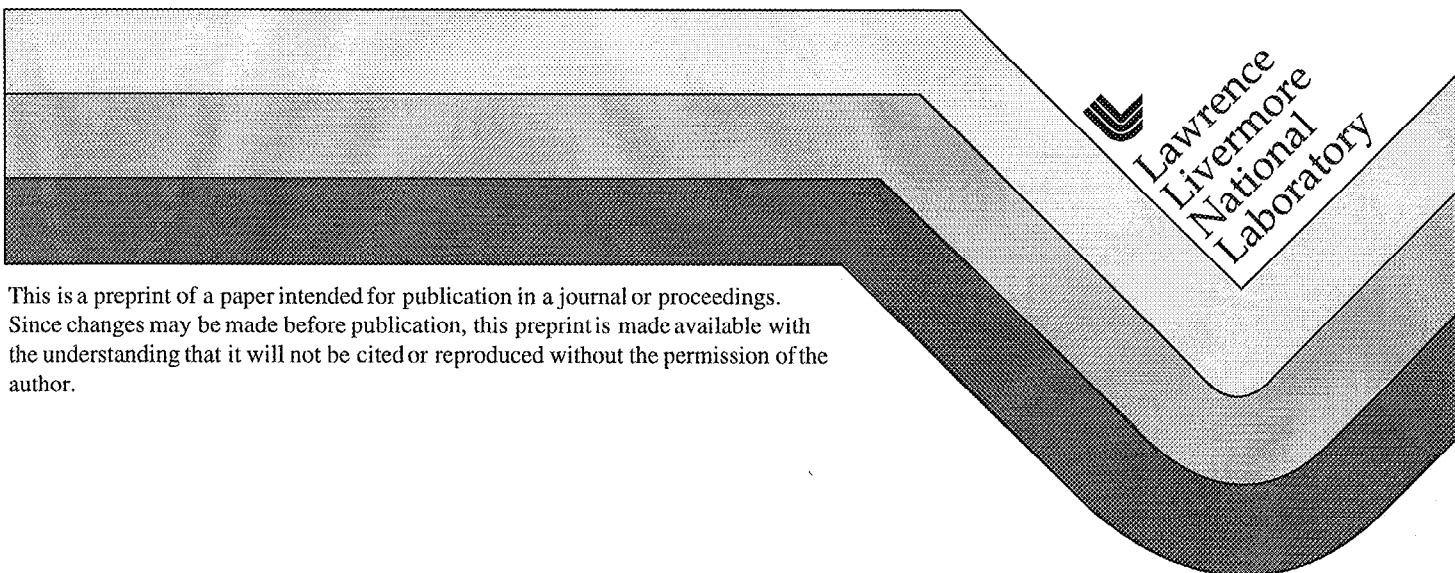
PREPRINT

# Edge and Coupled Core/Edge Transport Modeling in Tokamaks

L. L. Lodestro, T. A. Casper, R. H. Cohen, N. Mattor, L. D. Pearlstein, G. D. Porter,  
M. E. Rensink, T. D. Rognlien, D. D. Ryutov, H. A. Scott, A. S. Wan

This paper was prepared for submittal to the  
17th International Atomic Energy Agency Fusion Energy Conference  
Yokohama, Japan  
October 19-24, 1998

October 14, 1998



#### DISCLAIMER

This document was prepared as an account of work sponsored by an agency of the United States Government. Neither the United States Government nor the University of California nor any of their employees, makes any warranty, express or implied, or assumes any legal liability or responsibility for the accuracy, completeness, or usefulness of any information, apparatus, product, or process disclosed, or represents that its use would not infringe privately owned rights. Reference herein to any specific commercial product, process, or service by trade name, trademark, manufacturer, or otherwise, does not necessarily constitute or imply its endorsement, recommendation, or favoring by the United States Government or the University of California. The views and opinions of authors expressed herein do not necessarily state or reflect those of the United States Government or the University of California, and shall not be used for advertising or product endorsement purposes.

L.L. LODESTRO, T.A. CASPER, R.H. COHEN, N. MATTOR,  
L.D. PEARLSTEIN, G.D. PORTER, M.E. RENSINK, T.D. ROGNLIEN,  
D.D. RYUTOV, H.A. SCOTT, and A.S. WAN  
Lawrence Livermore National Laboratory  
P. O. Box 808, Livermore, CA 94551, USA

## Abstract

Recent advances in the theory and modelling of tokamak edge, scrape-off-layer and divertor plasmas are described. The effects of the poloidal  $E \times B$  drift on inner/outer divertor-plate asymmetries within a 1D analysis are shown to be in good agreement with experimental observations; above a critical  $v_{E \times B}$ , the model predicts transitions to supersonic SOL flow at the inboard midplane. Two-dimensional simulations show the importance of  $E \times B$  flow in the private-flux region and  $\nabla B$ -drift effects. A theory of rough plasma-facing surfaces is given, and interesting effects, some traveling back up the magnetic field-lines to the SOL plasma, are predicted. The parametric dependence of detached-plasma states in slab geometry has been explored; with sufficient pumping, the location of the ionization front can be controlled; otherwise only fronts at the plate or the X-point are stable. Studies with a more accurate Monte-Carlo neutrals model and a detailed non-LTE radiation-transport code indicate various effects are important for quantitative modelling. Long-lived oscillatory UEDGE solutions in both ITER and DIII-D are reported. Detailed simulations of the DIII-D core and edge are presented; impurity and plasma flow are shown to be well modelled with UEDGE, and the roles of impurity and neutral transport in the edge and SOL are discussed.

## 1. INTRODUCTION

Comprehensive modelling of the scrape-off-layer (SOL) plasma in a tokamak is a central issue for the design of high-power machines. The SOL's importance lies in its roles in plasma/wall interactions, ash and impurity control, and interactions with the edge plasma (i.e., the outermost closed flux-surfaces). In this paper we describe theoretical and simulation advances in modelling edge and SOL plasmas and make detailed comparisons with recent experimental measurements in the DIII-D tokamak. We present enhanced-performance core-transport scenarios for DIII-D, for which edge conditions and modelling are particularly important, and report the results of self-consistently coupled core/edge calculations.

## 2. PARTICLE-DRIFT EFFECTS IN THE EDGE AND SOL

### 2.1. In/out divertor-plate asymmetries produced by the $E \times B$ drift; 1D model

It has been noticed experimentally that the change of the toroidal magnetic field can considerably affect the distribution of particle and heat fluxes between the inner and the outer divertor plates [1]. A possible candidate responsible for this effect is the poloidal  $E \times B$  drift caused by the outward radial electric field that is always present in the open-field-line region [2]. Its origin is related to the sheath boundary conditions at the divertor plates and the fact that the electron temperature decreases with distance from the separatrix. As was pointed out in [3], the drift is directed towards the outer plate for the "normal" orientation of the toroidal magnetic field (when the ion drift is directed towards the plates), and changes sign with the reversal of the toroidal field. It is therefore tempting to attribute experimental trends to the presence of the poloidal drift. The observed trends in the heat flux asymmetry correlate well with the direction of the poloidal drift. However, the analysis of the particle fluxes on the open field lines carried out in paper [4] for a model of a uniform magnetic field has shown that the density and pressure asymmetry apparently anticorrelates with the experimental trend. On this basis, a conclusion was drawn in paper [5] that poloidal  $E \times B$  drifts cannot be responsible for

---

\* Work performed for USDOE under contract W-7405-ENG-48 at LLNL.

the experimentally observed correlations. In the present work we find that, if one uses a more realistic model of the plasma flow, one reaches agreement with experimentally observed trends even in 1D (2D effects discussed later further add to the trend). An important point of our analysis is the observation that the cross-section of the flux tube connecting two divertor plates is minimum on the inner-most side of the magnetic surface, thereby creating the geometry of a Laval nozzle for the plasma flow on its way to the inner strike point [6]. This, in turn, leads to the possibility that the plasma flow on the inner strike point becomes supersonic [4]. The second component of a more realistic picture is the presence of a temperature difference between the strike points caused by the much larger surface area of the outer part of the last closed flux surface compared to its inner part. Because of this, even in the absence of drifts, the heat flux to the outer strike point must be larger than that to the inner strike point [7]. When one imposes a poloidal drift on the plasma flow of this type, one recovers all experimentally observed correlations [8]. As an example, Fig. 2.1 demonstrates the dependence of the in/out density asymmetry vs. the poloidal drift-velocity for a temperature asymmetry between the strike points  $T_{\text{in}}/T_{\text{out}} = 0.4$ , and mirror ratio along the flux-tube  $R = 1.5$ . Effects of the radial drifts also give rise to the experimentally observed correlations [5,9]. What we would like to emphasize is that the poloidal drifts are at least as important.

## 2.2. 2D drift effects in the UEDGE code

For full 2D modeling of the edge and SOL we evolve the plasma and neutral densities, electron and ion temperatures, plasma potential, and ion and neutral parallel velocities within the UEDGE transport code [10]. A new element for the self-consistent plasma potential model is to include currents from both anomalous viscosity and classical  $\nabla B$  drifts in the current continuity equation. The anomalous radial current is obtained within a consistent ordering of the classical transport equations, using an enhanced collisionality to model turbulence while maintaining all intrinsic symmetries. Alternatively, the toroidal transport equations are rederived including fluctuations, with quasilinear closures for the anomalous terms. Both models give a 4<sup>th</sup>-order radial differential equation for the potential which can be used both inside the separatrix, where radial force balance is crucial, and outside the separatrix, where parallel currents dominate. Classical  $\nabla B$  drifts also make important contributions to the current, while the current from charge-exchange collisions near the separatrix is typically small for DIII-D parameters using the calculated neutral density. The resulting radial electric field has large shear near the separatrix as shown in Fig. 2.2 which should help stabilize edge/SOL turbulence.

The electric field also drives important  $E \times B$  transport flows. In addition to the  $\mathbf{v}_{B \times B}$  poloidal flows in the SOL obtained from the 1D model discussed earlier, a 2D effect is the  $\mathbf{v}_{B \times B}$  flow under the X-point in the private flux region. This flow enhances the inner-plate density for the ion  $\nabla B$  drift toward the X-point and decreases this density for a reversed  $B_{\text{tor}}$ . This effect makes inner-leg plasma detachment obtainable at lower gas-puff rate for normal  $B_{\text{tor}}$  direction than in the reversed direction, in agreement with DIII-D observations and is also consistent with Alcator C-Mod measurements [1]. Also, the change in profile shape plate current between normal and reversed  $B_{\text{tor}}$  obtained from probe measurements on JET [12] are qualitatively reproduced by our calculations.

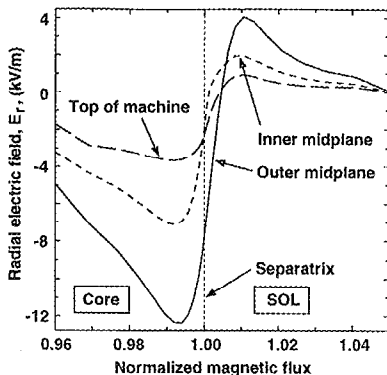


Fig. 2.1. Poloidal asymmetry in divertor-plate density vs. normalized poloidal electric drift velocity.

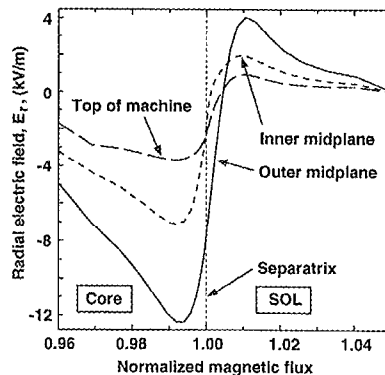


Fig. 2.2. UEDGE-calculated  $E_r$  at three poloidal locations for a low-power DIII-D case with ion  $\nabla B$  drift toward the X-pt. (There is a 2<sup>nd</sup> X-pt. near the top of the SOL.)

### 3. SHEATH OVER A SURFACE WITH SMALL-SCALE IMPERFECTIONS

The surface of a divertor plate typically has fine “topographic” structure determined by the intrinsic properties of the material (like the grainy structure of graphite), and by erosion processes. The characteristic size of the surface imperfections may vary over a broad range. The magnetic field intersects the divertor plate at a shallow angle  $\alpha \ll 1$ . We show that the presence of fine surface structures, together with the smallness of  $\alpha$ , gives rise to many interesting new phenomena in the sheath (the case of smooth waviness of the surface was considered in Ref. [13]). We assume that the surface is formed by the randomly distributed cones of height  $h$ , with base radius and the distance between neighboring cones both also of order  $h$ . This latter assumption means that the number of cones per unit surface area is  $\sim 1/h^2$ . We solve the problem in two steps: first assume that the electric field does not have a significant effect on the particle motion, and then consider possible complications. It turns out that, at small  $\alpha$ ’s, the plasma stream is entirely absorbed near the tops of the cones, so that the fraction of the rough surface “wetted” by plasma particles is small. In other words, the local heat and particle flux near the tips of the cones is much higher than for a flat divertor plate. Using general scaling arguments [14,15], one can find expressions for the fraction of the surface wetted by electrons and ions as a function of two parameters,  $\alpha$  and  $\rho_i/h$  (Fig. 2 and Table 1). One can see that, in a number of cases, the fraction of the surface “wetted” by the electrons is much less than that wetted by the ions. This in turn means that, because of a quasineutrality constraint, strong potentials will be formed to prevent the ions from entering the zones inaccessible for electrons. Projecting along the magnetic field lines into the bulk plasma, this fine potential structure will cause additional plasma diffusion towards the walls. In quasi-steady-state devices, a gradual ionization of the neutrals will create the neutralizing background of a cold plasma that will restore the picture described by Table 1, with different fractions of the surface wetted by electrons and ions.

### 4. TOPICS IN UEDGE MODEL DEVELOPMENT AND EDGE/SOL STUDIES

#### 4.1. Detached plasma states; Monte-Carlo neutrals effects

To minimize the heat load on divertor plates it is desirable to operate with detached plasmas, but there is some evidence [portersim] that a fully detached plasma evolves in time to an X-point MARFE with degraded core confinement. We have generated a detailed map of stationary solutions for the edge plasma as a function of various input parameters, e.g., the core plasma density, input power to the scrape-off-layer, and particle pumping at the divertor plate and sidewalls. We use the UEDGE code [10], with fluid models for both plasma and neutrals, in a Cartesian box geometry that simulates one quadrant of a single-null divertor configuration. We find stable solutions for all core plasma densities and powers when the sidewalls of the divertor are pumping surfaces. When there is no pumping, stable thermally-attached plasma solutions exist above some minimum input power; at lower power, stable strongly-detached solutions exist, but the plasma ionization front is near the X-point and may evolve to an X-point MARFE in a more realistic simulation geometry. There are additional stable and unstable solutions for some range of input powers; these correspond to varying degrees of thermal detachment with the ionization front at some intermediate point between the divertor plate and X-point. The stationary unstable solutions, when perturbed, evolve to a strongly detached plasma state.

To assess the range of validity of the inertial fluid neutrals model [16] in UEDGE, we compare results for similar problems run with the UEDGE fluid plasma model coupled to a Monte-Carlo [18] neutrals model. The test problem geometry is a Cartesian box that simulates one quadrant of a single-null divertor configuration.

We observe qualitatively similar results from the two models over a range of input powers where the plasma makes a transition between attached and detached states. The the Monte-Carlo neutrals model, with molecules, produces detached plasmas at somewhat higher input power than the fluid neutrals model. A point of disagreement is that without particle pumping at the sidewalls, no stable plasma states have been found with the Monte Carlo model, whereas a continuum of attached and detached states is found with the fluid neutrals model.

The most significant physics difference in the two neutrals models is in the recycling of particles absorbed at the divertor plate: the standard Monte Carlo model recycles them as thermal molecules at the wall temperature whereas the fluid model recycles them as thermal atoms at the local plasma ion temperature. For a detached plasma the mean free path of the molecules is comparable to the dimensions of the detached region because the electron temperature is less than 2 eV. This results in a nearly uniform molecular density in the detached region. The fluid model yields a much higher atomic density with a maximum at the divertor plate. The mechanism for transporting recycled particles from the divertor plate upstream to the ionization front is quite different in the two models: molecules stream freely through the detached region while atoms diffuse upstream via charge exchange with the plasma background. The plasma sources/sinks for particles and electron thermal energy from the two neutrals models agree within about 20%, but the sources/sinks for ion parallel momentum and ion thermal energy are grossly different. The primary mechanism for ion momentum and ion thermal energy transfer is charge exchange and this is relatively much weaker in the Monte Carlo model because molecules are the dominant species.

When the Monte Carlo model is run in a mode which closely matches the physics assumptions of the fluid neutrals model (no molecules), one finds good agreement on the radially-averaged plasma sources and neutral densities from the two models with a fixed detached background plasma.

## 4.2. Radiation transport

We have estimated the effect of radiation trapping in UEDGE on detached divertor plasmas in ITER including multi-species neon and carbon. The energy loss from (initially dominant) hydrogen radiation is locally suppressed by a factor, while the transport associated with the 13.6 eV loss of electron energy during ionization and its subsequent partial redeposition upon recombination is retained. In optically thick detached plasmas, increasing only the suppression factor results in a poloidal broadening of the ionization front and a shift of radiation from hydrogen to carbon such that the detached state is maintained. More detailed calculations performed with CRETIN, a full radiation transport code, using plasma profiles from UEDGE, are compared to DIII-D spectral measurements.

## 4.3. Limit cycles and long-time behavior of SOL plasmas

Long-lived oscillatory UEDGE solutions have been found in partially detached divertor plasmas, especially with a fixed-fraction neon impurity. The cooling caused by neon radiation near the X-point and the neutral gas impinging from the private flux region couple out of phase to drive the oscillation. When the impurity charge-states are fully transported, however, the oscillations slowly damp. The parametric dependence of the stable/damped boundary is investigated. We find that long-lived  $\sim 10$  ms oscillations, in conjunction with very low plate densities, can also occur with the more realistic sputtering models recently installed in UEDGE for DIII-D simulation (see below).

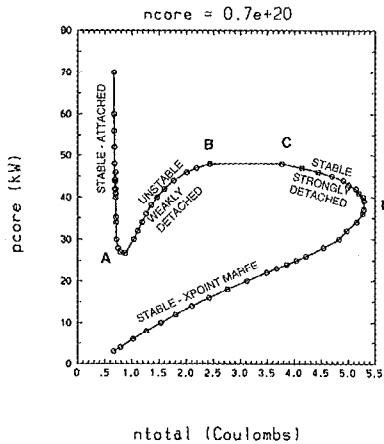


Fig. 4.1. caption

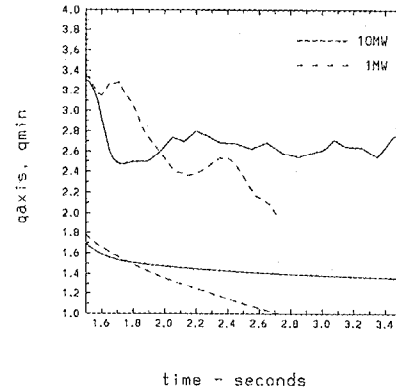


Fig. 5.1.1. Temporal variation of  $q_{axis}$  and  $q_{min}$  for simulated ECH powers of 1 & 10 MW with  $q_{min}$  sustained for  $25 \tau_E$  at 10 MW.

## 5. PROGRESS AND DIRECTIONS IN DIII-D SIMULATIONS

### 5.1. High-performance core modelling with Corsica

Using a combination of heating and current drive during the Ohmic current ramp-up leads to the formation of discharges with negative central shear (NCS). In several experiments; e.g. DIII-D, TFTR, JET and JT60U, these NCS configurations have resulted in very high performance operation exhibiting some of the highest normalized beta ( $\beta_N$ ) and neutron production rates in the DIII-D tokamak [19]. The difficulty with these advanced tokamak discharges is to extend their transient performance to long pulse lengths and ultimately to steady-state discharges at high  $\beta_N$ . This requires active control of heating, fueling and current-drive systems. For discharges representative of DIII-D operation, we are modelling the affects of electron cyclotron heating (ECH) and current drive (ECCD) to explore methods to extend the duration of high performance and to broaden the region of negative shear. Time-dependent CORSICA simulations using a transport model coupling the minimum of  $q$  to the location of the transport barrier have been done [20]. These simulations indicate that at sufficiently high power ( $>$  few MW absorbed), the barrier can be sustained for several energy-confinement times,  $\tau_E$ , as indicated in Fig. 5.1.1, where the position of  $q_{\min}$  was maintained for  $\sim 25 \tau_E$ . In many of these experiments on DIII-D, we control the pressure profile peaking by control of L-to-H-mode transitions by biasing the plasma position. This is important for controlling disruptions while maintaining high performance. The core/edge coupling in CORSICA 2 is being developed as a tool to model these effects for high-performance discharges like NCS.



## 5.2. Modelling the DIII-D edge and SOL with UEDGE

The UEDGE code has been validated against a large variety of data from the DIII-D tokamak in the past, including radial profiles of the plasma density and temperature at the outer midplane, 2-D profiles of the plasma density and temperature in the divertor region, bolometric measurements of the total radiation profiles, and profile measurements of  $D_\alpha$  emission [21–24]. Recent improvements in the code have permitted inclusion of the effect of intrinsic carbon impurities introduced to the SOL with realistic models for both chemical and physical sputtering [25,26]. Two diagnostics are useful in efforts to validate these code improvements: the bolometric measurement of total radiated power, and measurement of the parallel flow velocity of both the impurity ions and the primary flow ions [27–29]. The radiation pattern is determined by a combination of the source distribution of the carbon impurities, and the radial and parallel transport of each of the ionization states of the impurities, together with detailed atomic physics of ionization, recombination, and charge exchange. We assume anomalous radial diffusion in UEDGE, and use a spatially constant diffusivity for all ion species. The parallel transport of impurity ions is obtained by force balance, using the impurity forces proposed by Keilhacker [30]. We find the dominant forces on the ions to be drag on the hydrogenic fuel ions and  $\nabla T_i$  forces which move the impurities up the ion temperature gradient. The parallel flow velocities of both the fuel ions and the  $C^+$  ion species predicted by the UEDGE model are consistent with the new measurements, as shown in Fig. 5.2.1. This figure compares the simulation and measured Mach number of the primary ion flow measured along a vertical line just outside the outer strike point in (a), and the parallel velocity of  $C^+$  ions along a line which views the plasma essentially tangential to a surface lying just outside the X-point in (b). The  $C^+$  ion velocity is measured spectroscopically, permitting determination of positive and negative flow components at different radii. A positive velocity is toward the outer plate, and a negative velocity is away from the plate. Similar agreement has been obtained for a discharge in which the outer leg is detached by injection of additional  $D_2$  gas, and for a discharge with the outer strike point moved outward radially permitting diagnosis of the inner leg of the divertor.

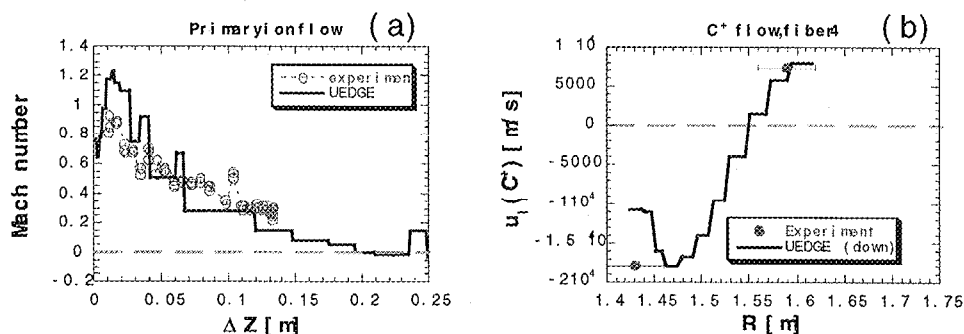


Fig. 5.2.1. Comparison of simulated and measured flows for the primary ions (a) and singly ionized carbon (b) in DIII-D.

The agreement between the UEDGE simulation and the measured flow velocities indicates the impurity behavior in DIII-D follows classical parallel physics. A simple model diffusion coefficient for radial transport is consistent with the data. This classical model is consistent with measurement for attached and detached plasmas on both the inner and outer divertor legs. The UEDGE model permits examination of the question of impurity transport from the walls of DIII-D to the closed flux surfaces. Typically we find impurity buildup of the  $C^{+4}$  ionization state at a force null in which the net force on the  $C^{+4}$  ion is toward the null from either side. The position of this null is determined by details of the parallel ion temperature profile and the flow pattern of the fuel ion species. The  $C^{+4}$  ion density builds up to a high level in the SOL, then diffuses into the core where the carbon is quickly ionized to higher states. These results are shown in Fig. 5.2.2.

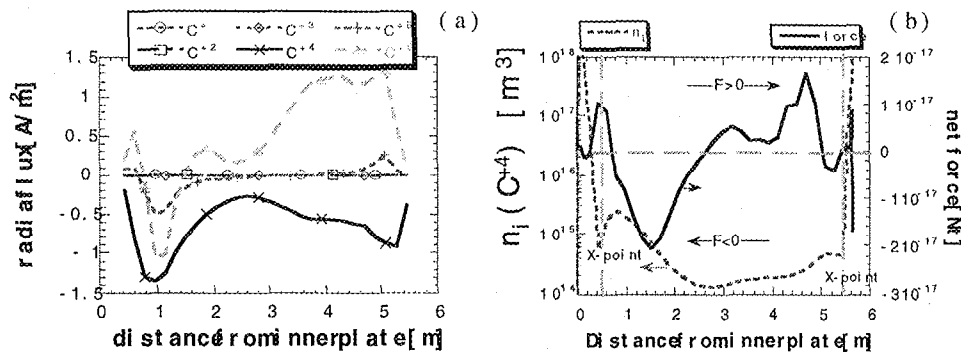


Fig. 5.2.2. The poloidal variation of the radial particle flux of impurity ionization states (a), and the density and net force on a  $C^{+4}$  ion (b).

### 5.3. Core/edge coupling

Edge profile conditions play a crucial role in the high-performance regimes described above. In L-mode, central pressure peaking can cause disruptions, whereas H-mode profiles can prevent sufficient beam penetration and support steep edge pressure-gradients which drive currents resulting in ELMS. Both in order to assess our ability to experimentally control profiles by inducing L/H transitions, and in order to analyse the underlying interplay of edge physics and core confinement, LLNL's core/edge coupling code CORSICA 2 [31] is being extended and validated against DIII-D. CORSICA 2 couples the core transport code CORSICA 1 to UEDGE in a fully self-consistent manner, such that UEDGE can be run either in time-dependent mode or in quasi-static equilibrium with the shared boundary condition at the outer core. Coupled fields include  $n_D$ ,  $n_\alpha$ ,  $T_e$ ,  $T_i$ ,  $n_{gas}$ , and toroidal momentum. With the addition of an SOL-turbulence-driven transport coefficient [32] to UEDGE, we have simulated an L/H transition in DIII-D, with profiles in qualitative agreement with experiment.

### References

- [1] HUTCHINSON, I.H., LABOMBARD, B., GOETZ, J.A., et al., Plasma Phys. and Contr. Fusion **37** (1995) 1389.
- [2] STANGEBY, P.C., MCCracken, G.M., Nucl. Fus. **30** (1990) 1225.
- [3] TENDLER, M., ROZHANSKY V., Comm. on Plasma Phys. and Contr. Fus. **13** (1991) 191.
- [4] COHEN, R.H., RYUTOV, D.D., Comm. on Plasma Phys. and Contr. Fus. **16** (1995) 255.
- [5] CHANKIN, A.V., J. Nucl. Materials **241-243** (1997) 199.
- [6] RYUTOV, D.D., Contrib. Plasma Phys. **36** (1996) 207.
- [7] HARBOUR, P.J. et al., Contrib. Plasma Phys. **28** (1988) 417.
- [8] COHEN, R.H., RYUTOV, D.D., Sherwood Theory Conference, Atlanta, March 1998.
- [9] STANGEBY, P.C., CHANKIN, A.V., Nucl. Fusion, **36** (1998) 839.
- [10] ROGNLIEN, T.D., MILOVICH, J.L., RENSINK, M.E., and PORTER, G.D., "A fully implicit, time dependent 2-D fluid code for modeling tokamak edge plasmas," J. Nucl. Mat. **196-198** (1992) 347.
- [11] ROGNLIEN, T.D., BROWN, P.N., CAMPBELL, R.B., et al., Contrib. Plasma Phys. **34** (1994) 362.
- [12] SCHAFFER, M.J., CHANKIN, A.V., GUO, H.Y., et al., Nucl. Fusion **37** (1997) 83.
- [13] COHEN, R.H., RYUTOV, D.D., Nucl. Fusion **37** (1997) 621.
- [14] COHEN, R.H., RYUTOV, D.D., Phys. Plasmas **5** (1998) 2194.
- [15] COHEN, R.H., et al., J. Nucl. Materials, to be published.
- [16] WISING, F., KNOLL, D.A., KRASHENINNIKOV, S.I., ROGNLIEN, T.D. and SIGMAR, D.J., "Simulation of Detachment in ITER Geometry Using the UEDGE Code and a Fluid Neutral Model," Contr. Plasma Phys. **36** (1996) 309.
- [17] KRASHENINNIKOV, S.I., RENSINK, M., ROGNLIEN, T., et al., J. Nucl. Materials, to be pub., 1999.

- [18] REITER, D., "Progress in two-dimensional plasma edge modelling," J. Nucl. Mat. **196–198** (1992) 80.
- [19] RICE, B.W. et al., Nucl. Fus. **36** (1996) 1271.
- [20] CASPER, T.A. et al., to be published in the Proceedings of the 25th EPS Conference on Controlled Fusion and Plasma Physics, Prague, Czech Republic (1998).
- [21] PORTER, G.D., ALLEN, S.L., BROWN, M., FENSTERMACHER, M.E., et al., "Simulation of experimentally achieved DIII-D detached plasmas using the UEDGE code," Phys. Plasmas **3**(5) (1996) 1967.
- [22] PORTER, G.D., FENSTERMACHER, M., GROEBNER, R., LEONARD, A., et al., "Benchmarking UEDGE with DIII-D Data," Contrib. Plasma Phys. **34**(2/3) (1994) 454–459.
- [23] FENSTERMACHER, M.E., ALLEN, S.L., BROOKS, N.H., BUCHENAUER, D.A., et al., "The Two-dimensional structure of radiative divertor plasmas in the DIII-D tokamak," Phys. Plasmas **4**(5) (1997) 1761.
- [24] FENSTERMACHER, M.E., PORTER, G.D., RENSINK, M.E., ROGNLIEN, T.D., et al., "UEDGE and DEGAS Modeling of the DIII-D Scrape-off Layer Plasma," J. Nucl. Mater. **220–222** (1995) 330.
- [25] DAVIS, J.W., and HAASZ, A.A., "Impurity release from low-Z materials under light particle bombardment," J. Nucl. Mater. **241–243** (1997) 37–51.
- [26] DAVIS, J.W., HAASZ, A.A., and STANGEBY, P.C., "Hydrocarbon formation due to Combined H<sup>+</sup> ion and H<sup>0</sup> atom Impact on Pyrolytic Graphite," J. Nucl. Mater. **155–157** (1988) 234–240.
- [27] ISLER, R.C., BROOKS, N.H., WEST, W.P., LEONARD, A.W., et al., "Normal and Reversed Impurity Flows in the DIII-D Divertor," submitted to Phys. Plasmas (1998).
- [28] ISLER, R.C., BROOKS, N.H., LEONARD, A.W., and WEST, W.P., "Spectroscopic Measurements of Ion Temperatures and Parallel Flows in the DIII-D Divertor," to be published in J. Nucl. Mater. (1998).
- [29] BOEDO, J., PORTER, G.D., SCHAFFER, M., LEHMER, R., et al., "Flow Reversal, Convection and Modeling in the DIII-D Divertor," accepted by Phys. Plasmas (1998).
- [30] KEILHACKER, M., SIMONINI, R., TARONI, A., and WATKINS, M.L., "Scrape-off layer model for the study of impurity retention in the pumped divertor planned for JET," Nucl. Fus. **31**(3) (1991) 535.
- [31] TARDITI, A. et al., "Self-consistent core/edge nonlinear transport simulations with Corsica 2," Contrib. Plasma Phys. **36** (1996) 132.
- [32] COHEN, R.H., and XU, X.Q., Phys. Plasmas **2** (1995) 3374.